Structural long period gratings made by drilling micro-holes in photonic crystal fibers with a femtosecond infrared laser

Shujing Liu, Long Jin, Wei Jin*, Dongning Wang, Changrui Liao, Ying Wang

Department of Electrical Engineering, The Hong Kong Polytechnic University, Hung Hom, Kowloon, Hong Kong, P. R. China
**eewjin@polyu.edu.hk*

Abstract: We present a new method for fabricating structural long-period gratings (LPGs) in photonic-crystal fibers (PCFs). The method is based on periodically drilling holes into the PCF cladding along the length of the fiber by use of a focused femtosecond infrared laser. A very short LPG with only 9 periods and a grating length of < 4 mm exhibited resonance strength of over 20 dB and a polarization dependent loss of 25 dB. The high resonance strength is attributed to the strong modulated mode-field profile caused by the significant perturbation of the fiber geometry. The mechanism of LPG formation is discussed based on coupled local-mode theory.

©2010 Optical Society of America

OCIS codes: (060.2310) Fiber optics; (220.4000) Microstructure fabrication (050.2770) Gratings; (060.4005) Microstructured fibers.

References and links

1. A. M. Vengsarkar, P. J. Lemaire, J. B. Judkins, V. Bhatia, T. Erdogan, and J. E. Sipe, "Long period fiber gratings as band rejection filters," J. Lightwave Technol. **14**(1), 58–65 (1996).
2. S. W. James, and R. P. Tatam, "Optical fibre long-period grating sensors: characteristics and application," Meas. Sci. Technol. **14**(5), R49–R61 (2003).
3. S. Savin, M. J. F. Digonnet, G. S. Kino, and H. J. Shaw, "Tunable mechanically induced long-period fiber gratings," Opt. Lett. **25**(10), 710–712 (2000).
4. Y. P. Wang, D. N. Wang, W. Jin, Y. J. Rao, and G. D. Peng, "Asymmetric long period fiber gratings fabricated by use of CO_2 laser to carve periodic grooves on the optical fiber," Appl. Phys. Lett. **89**(15), 151105 (2006).
5. G. Rego, O. Okhotnikov, E. Dianov, and V. Sulimov, "High-temperature stability of long-period fiber gratings produced using an electric arc," J. Lightwave Technol. **19**(10), 1574–1579 (2001).
6. J. S. Petrovic, H. Dobb, V. K. Mezentsev, K. Kalli, D. J. Webb, and I. Bennion, "Sensitivity of LPGs in PCFs fabricated by an electric arc to temperature, strain, and external refractive index," J. Lightwave Technol. **25**(5), 1306–1312 (2007).
7. H. Dobb, K. Kalli, and D. J. Webb, "Temperature insensitive long period grating sensors in photonic crystal fibre," Electron. Lett. **40**(11), 657–658 (2004).
8. H. Dobb, K. Kalli, and D. J. Webb, "Measured sensitivity of long period gratings in photonic crystal fibre," Opt. Commun. **260**, 184–191 (2006).
9. G. Kakarantzas, T. A. Birks, and P. St. J. Russell, "Structural long-period gratings in photonic crystal fibers," Opt. Lett. **27**(12), 1013–1015 (2002).
10. Y. P. Wang, L. M. Xiao, D. N. Wang, and W. Jin, "Highly sensitive long-period fiber-grating strain sensor with low temperature sensitivity," Opt. Lett. **31**(23), 3414–3416 (2006).
11. C. Kerbage, and B. J. Eggleton, "Tunable microfluidic optical fiber gratings," Appl. Phys. Lett. **82**(9), 1338–1340 (2003).
12. S. J. Mihailov, C. W. Smelser, D. Grobnic, R. B. Walker, P. Lu, H. Ding, and J. Unruh, "Bragg gratings written in all-SiO_2 and Ge-doped core fibers with 800-nm femtosecond radiation and a phase mask," J. Lightwave Technol. **22**(1), 94–100 (2004).
13. A. Martinez, M. Dubov, I. Khrushchev, and I. Bennion, "Photoinduced modifications in fiber gratings inscribed directly by infrared femtosecond irradiation," IEEE Photon. Technol. Lett. **18**(21), 2266–2268 (2006).
14. S. J. Mihailov, D. Grobnic, C. W. Smelser, P. Lu, R. B. Walker, and H. Ding, "Induced Bragg gratings in optical fibers and waveguides using an ultrafast infrared laser and a phase mask," Laser Chem. **2008**, 416251 (2008).
15. C. B. Schaffer, A. Brodeur, and E. Mazur, "Laser-induced breakdown and damage in bulk transparent materials induced by tightly focused femtosecond laser pulses," Meas. Sci. Technol. **12**(11), 1784–1794 (2001).
16. Y. Kondo, K. Nouchi, T. Mitsuyu, M. Watanabe, P. G. Kazansky, and K. Hirao, "Fabrication of long-period fiber gratings by focused irradiation of infrared femtosecond laser pulses," Opt. Lett. **24**(10), 646–648 (1999).

#119793 - $15.00 USD Received 10 Nov 2009; revised 25 Dec 2009; accepted 4 Jan 2010; published 3 Mar 2010
(C) 2010 OSA

17. T. Allsop, K. Kalli, K. Zhou, G. Smith, Y. Lai, M. Dubov, K. Sugden, D. Webb, I. Bennion, and M. Komodromos, "Characterisation of femtosecond laser inscribed long period gratings in photonic crystal fibre," Proc. SPIE **6990**, 1–13 (2008).
18. T. Allsop, K. Kalli, K. Zhou, Y. Laia, G. Smith, M. Dubov, D. J. Webb, and I. Bennion, "Long period gratings written into a photonic crystal fibre by a femtosecond laser as directional bend sensors," Opt. Commun. **281**(20), 5092–5096 (2008).
19. C. J. Hensley, D. H. Broaddus, C. B. Schaffer, and A. L. Gaeta, "Photonic band-gap fiber gas cell fabricated using femtosecond micromachining," Opt. Express **15**(11), 6690–6695 (2007).
20. A. van Brakel, C. Grivas, M. N. Petrovich, and D. J. Richardson, "Micro-channels machined in microstructured optical fibers by femtosecond laser," Opt. Express **15**(14), 8731–8736 (2007).
21. Y. Zhu, P. Shum, H.-W. Bay, M. Yan, X. Yu, J. Hu, J. Hao, and C. Lu, "Strain-insensitive and high-temperature long-period gratings inscribed in photonic crystal fiber," Opt. Lett. **30**(4), 367–369 (2005).
22. G. Humbert, A. Malki, S. Février, P. Roy, and D. Pagnoux, "Characterizations at high temperatures of long-period gratings written in germanium-free air-silica microstructure fiber," Opt. Lett. **29**(1), 38–40 (2004).
23. C. L. Zhao, L. Xiao, J. Ju, M. S. Demokan, and W. Jin, "Strain and temperature characteristics of a long-period grating written in a photonic crystal fiber and its application as a temperature-insensitive strain sensor," J. Lightwave Technol. **26**(2), 220–227 (2008).
24. B. L. Bachim, and T. K. Gaylord, "Polarization-dependent loss and birefringence in long-period fiber gratings," Appl. Opt. **42**(34), 6816–6823 (2003).
25. A. W. Snyder, and J. D. Love, *Optical Waveguide Theory* (Chapman & Hall, New York, 1983).
26. T. Matsumura, T. Nakatani, and T. Yagi, "Deep drilling on a silicon plate with a femtosecond laser: experiment and model analysis," Appl. Phys., A Mater. Sci. Process. **86**(1), 107–114 (2006).

1. Introduction

In a long-period grating (LPG) the fundamental core mode is coupled resonantly to a series of cladding modes, resulting in attenuation dips in the transmission spectrum [1]. LPGs have been widely used in gain-flattening and fiber sensing [1, 2]. In conventional single-mode fibers (SMFs), LPGs may be inscribed through refractive-index modulation of the fiber core by ultraviolet (UV) exposure [1], lateral stress with a mechanical template [3], and heat treatment with a CO_2 laser or an electric arc [4–8]. For photonic-crystal fiber (PCFs), in addition, structural LPGs may be formed by periodically collapsing the air-holes in the cladding or filling liquids into the air-hole channels [9–11].

Recently, there have been considerable activities in fabricating fiber Bragg gratings in non-photosensitive silica fibers (e.g., PCFs) by use of focused femtosecond infrared (IR) laser pulses in combination with a phase mask [12], or a point-by-point writing technique [13]. Refractive-index modifications are induced by the local material densification due to multiphoton absorption of intense femtosecond IR pulses [12]. Depending upon the intensity of the femtosecond IR laser exposure, the refractive index changes can be considered due to a type I-IR (for intensity below the ionization threshold, which is ~3.2×10^{13} W/cm^2 for fused silica) or a type II-IR (for intensity above the ionization threshold) process [14, 15]. The gratings formed by the type II-IR process are permanent or "damage" gratings while the type I-IR gratings may be erased at elevated temperatures.

Many studies have demonstrated the ability to fabricate LPGs in SMFs and PCFs, which are made from intense IR exposure of intensity about 10^{14} W/cm^2 [16–18]. These LPGs may be regarded as more of "index-type" gratings since no significant modification of the waveguide geometry can be observed from the fiber surface. However, if the intensity of the femtosecond IR exposure is sufficiently high to induce ablation and material removal, permanent change of waveguide structure may result. An example of significant waveguide structural change is the micro-scale holes drilled into the fiber core of PCFs, which have been used as access paths for micro-fluidic or gas-related applications [19, 20]. In this paper, we demonstrate structural LPGs fabricated by use of a femtosecond IR laser to periodically drill micro-holes into the cladding of PCFs. This method minimizes the effect of IR light scattering by the air-columns within the PCFs and enhances the efficiency of LPG inscription. An over 20 dB resonance dip can be formed with only 10 periods, as a result of the significantly modified local-modes due to the strong perturbation of the waveguide geometry. Based on the coupled local-mode theory, we analyze the coupling behavior and spectral characteristics of this type of structural LPGs, which are supported by experimental results. The permanent structural LPGs in the pure silica PCFs are expected to have high thermal stability and of

#119793 - $15.00 USD Received 10 Nov 2009; revised 25 Dec 2009; accepted 4 Jan 2010; published 3 Mar 2010
(C) 2010 OSA

interest for use as devices and sensors for operation in high-temperature environments [21, 22]. The hole-drilling may also be used to fabricate fiber grating devices in other types of optical fibers.

2. Fabrication of LPGs in PCFs

The experimental setup for LPG fabrication is shown in Fig. 1. Femtosecond laser pulses with duration of 120 fs and repetition rate of 1 kHz were produced by a Ti: sapphire regenerative amplifier system (Spectra-Physics) with a central wavelength of 800 nm. The laser pulses with Gaussian beam radius of about 2 mm were focused onto the PCF by a microscope objective (×20, NA = 0.5, working distance = 2.1 mm) and the diffraction-limited focal spot diameter ($1/e^2$ of intensity) is estimated to be 2 μm. The intensity of the laser beam was controlled using a half-wave plate and a linear polarizer and neutral-density filters. The PCF was mounted on a computer-controlled three-axis translation stage with tuning resolution of 40 nm and repeatability of 300 nm. The exposure time was controlled with a mechanical shutter.

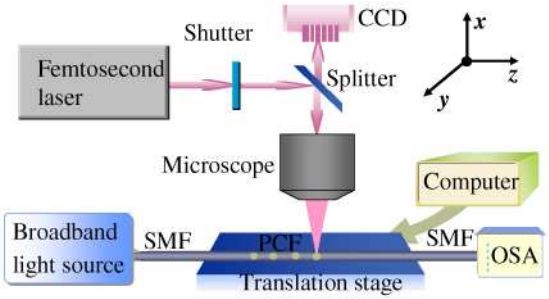

Fig. 1. Experiment setup for LPG fabrication.

A section of large mode area PCF (LMA-10 PCF, purchased from NKT Photonics) is spliced to conventional SMFs (SMF28) at both ends. The LMA-10 PCF is an endlessly single mode fiber with a mode area approximately matched to the SMF28 fibers. The specifications and the cross-section of the LMA-10 PCF can be found in reference [23]. The location of the focal point on the PCF can be accurately determined with the assistance of an optical microscope (Nikon 80i). The femtosecond laser (pulse energy of 5 μJ) was first focused on and aligned at the center of the fiber on its upper surface, and the focal point is then moved toward the fiber core with a speed of 5 μm/s by moving the fiber along the *x*-direction, as indicated in Fig. 1. The total moving length is ~ 60 μm from the surface to the fiber core. A micro-hole from fiber surface to fiber core was thus drilled. Figure 2 shows the morphology and depth of the hole. Figure 2(a) is the microscopic image taken from the top of a section of the LPG. Figure 2 (b) is the cross-sectional image taken with a scanning electron microscope (SEM), and Fig. 2(c) is the image of the drilled region taken from the side of the fiber. By using the same fabrication parameters, a number of almost identical holes were drilled along the fiber with a separation of 420 μm, thus creating an LPG in the PCF. During the fabrication process, the transmission spectrum was monitored by a broadband light source and optical spectrum analyzer (OSA), which were connected to the input and output SMF pigtails of the PCF sample, respectively.

The measured evolution of the transmission spectrum with increasing number of grating periods is shown in Fig. 3. The strength of the resonance dip at 1559 nm is over 20 dB in an LPG made of 10 holes, corresponding to a grating length of only 3.78 mm. This LPG has a much shorter length than the one reported in [18]. Obviously, our LPG is a "structural" grating resulted from significant modification of the fiber geometry, i.e., the drilled holes. To drill these holes, the intensity of the femtosecond IR exposure is very high, of the order of 10^{15} W/cm^2 (corresponding to 5 μJ pulse energy). Due to the stronger mode coupling in the drilled-hole region, the present LPG possesses higher coupling strength and hence shorter

#119793 - $15.00 USD Received 10 Nov 2009; revised 25 Dec 2009; accepted 4 Jan 2010; published 3 Mar 2010
(C) 2010 OSA

grating length. We measured the polarization-dependent loss (PDL) by using an Agilent 81910A photonic all-parameter analyzer with a wavelength resolution of 50 pm. The result is also shown in Fig. 3. The PDL is as large as 25 dB around the resonant wavelength. This is probably because the drilled holes introduced a very strong asymmetry in both the cladding and core geometries, which induces large asymmetrical mode-field profile and birefringence [24]. The LPGs we fabricated have reasonable mechanical strength and can withstand a maximum stain of 700 με before breaking. Near-field measurements were carried out to determine which cladding mode the fundamental mode couples into at the resonant wavelength. The measurements were realized by replacing the eyepiece of a microscope with an infrared camera and by use of a tunable laser (Agilent 8164B). Figure 4(a) shows the recorded near-field profile just after the 10th drilled-hole when the tunable laser is tuned to the resonant wavelength around 1559 nm. The image in Fig. 4(a) suggests that the fundamental mode is coupled to a LP_{11} like cladding mode and the cladding mode profile is asymmetric because of the strong perturbation of the waveguide geometry by the drilled-holes.

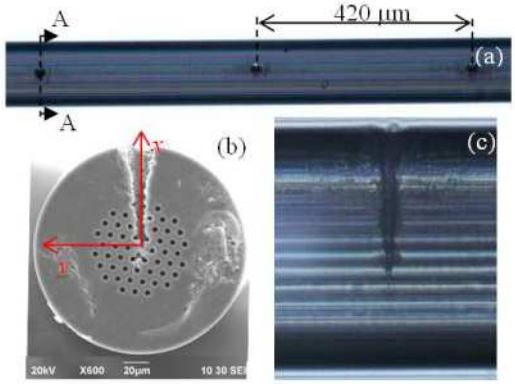

Fig. 2. (a) Top view of a section of the LPG in PCF. (b) SEM cross-sectional image of the drilled region, where the PCF is cut at the A–A plane in (a). (c) Side view of the drilled region.

We fabricated several LPGs with different periods. The measured resonant wavelength as function of the grating period is shown in Fig. 5 as solid red squares. The LPG with resonant wavelength of 1559 nm corresponds to the one with its spectrum shown in Fig. 3. The resonance wavelength blue shifts with increasing grating pitch, which agrees with the previously reported results of LPGs inscribed in a similar PCF [23]. We have also observed attenuation dips at the shorter wavelength side of the main LP_{11} dip, which are believed to be due to couplings into the higher-order cladding modes. These resonances are however much weaker than the LP_{11} mode resonance and not to be discussed in this paper.

#119793 - $15.00 USD Received 10 Nov 2009; revised 25 Dec 2009; accepted 4 Jan 2010; published 3 Mar 2010
(C) 2010 OSA

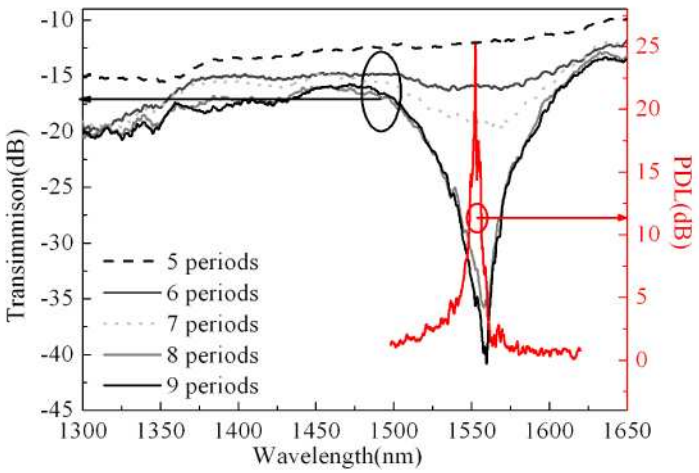

Fig. 3. Evolution of transmission spectra and the measured PDL profile of a LPG in PCF.

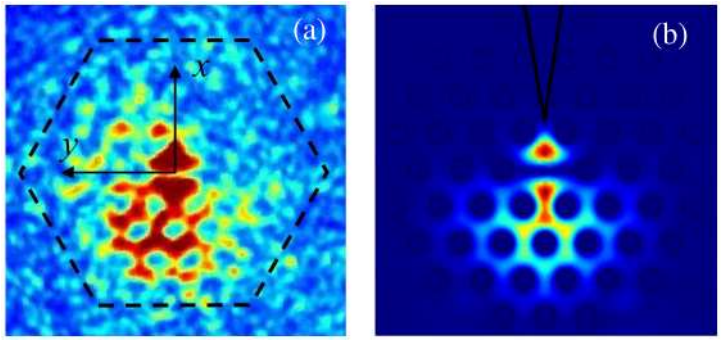

Fig. 4. Near-field intensity profiles at the resonant wavelength. (a) Measured at the output of the LPG by use of an infrared camera; (b) Calculated LP_{11} mode profile for the perturbed structure at location F as shown in Fig. 6(a).

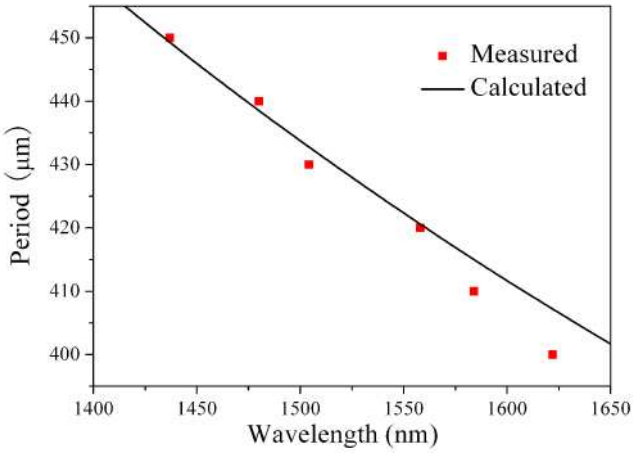

Fig. 5. The relationship between the LP_{01}-LP_{11} resonant coupling wavelength and the grating period. The parameters used for numerical calculation are: diameter of the air hole d = 3.38 μm, hole to hole spacing D = 7.31 μm, grating period Λ= 420 μm.

#119793 - $15.00 USD Received 10 Nov 2009; revised 25 Dec 2009; accepted 4 Jan 2010; published 3 Mar 2010
(C) 2010 OSA

3. Discussion

The femtosecond-laser-drilled LPG introduces large and abrupt structural modification in the laser-drilled region, typically of a few micrometers in diameter and ~ 60 μm in depth. This results in strong changes in the field of cladding modes. The conventional simplified coupled-mode theory is therefore not applicable here. Instead, coupled local-mode theory [25], which can be used to model the mode properties of waveguides with larger non-uniformities, is adopted here to study the effect of the drilled-holes. According to this theory, electric and magnetic fields in the fiber can be expressed by a superposition of local modes and radiation fields. The core mode is partially coupled into individual cladding modes and radiation modes when light propagates through the drilled-hole region. Although an individual local-mode is not an exact solution of Maxwell's equations for the unperturbed fiber, the individual local-modes in a set still satisfy the mode orthogonality. Considering only coupling between co-propagating modes, the coupling behavior between the core mode (LP_{01}) and a specific cladding mode, e.g., LP_{11} cladding mode, is expressed by [25]:

$$\begin{aligned} \frac{\mathrm{d}b_{\mathrm{co}}}{\mathrm{d}z} - i\beta_{\mathrm{co}}(z)b_{\mathrm{co}} &= C(z)\cdot b_{\mathrm{cl}} \\ \frac{\mathrm{d}b_{\mathrm{cl}}}{\mathrm{d}z} - i\beta_{\mathrm{cl}}(z)b_{\mathrm{cl}} &= -C(z)\cdot b_{\mathrm{co}} \end{aligned} \tag{1}$$

where b represents the magnetic or electric field of a mode, $\beta = \frac{2\pi}{\lambda}n$ is the propagation constant, and n is the mode effective index. The subscripts "*co*" and "*cl*" denote the core and cladding modes, respectively. $C(z)$ is the coupling coefficient that quantifies the efficiency of coupling between the core and cladding local-modes, which is defined by [25]

$$C = \frac{1}{4}\int_{A\infty}\left\{\overline{h_{\mathrm{co}}}\times\frac{\partial\overline{e_{\mathrm{cl}}}}{\partial z} - \overline{e_{\mathrm{co}}}\times\frac{\partial\overline{h_{\mathrm{cl}}}}{\partial z}\right\}\bullet\bar{z}\,\mathrm{d}A \tag{2}$$

Based on the SEM and the microscope images of the drilled-holes (e.g., Figs. 2(a) to (c)), we model the laser-drilled regions with idealized cone-shaped holes (the upper panel in Fig. 6(a)) and use this model to calculate the variation of coupling coefficient $C(z)$ along the fiber length. In this model, the full angle of the hole is 17 ° and the distance between the tip of the hole (i.e., location C) and the central axis of the fiber is 3.5 μm. The hole-region is divided into many sections with increment Δz along the longitudinal direction of the fiber. With an FEM software, the LP_{01} and LP_{11} local-mode fields are calculated for every sections and the coupling coefficient at different location along the fiber is then calculated by using Eq. (2). Fig. 4(b) shows the calculated LP_{11}-like local-mode intensity profile at position F (see Fig. 6(a)). The black triangle in the background of Fig. 4(b) shows the position of the drilled-hole. The intensity profile is clearly asymmetric due to the introduction of the hole, which agrees with the recorded image shown in Fig. 4(a). However, we would like to point out that Fig. 4(b) is not intended to be an accurate prediction of the image in Fig. 4(a), which is the result of a complex distributed coupling process and is difficult to predict accurately. The calculated variation of LP_{01}-LP_{11} coupling coefficient $C(z)$ is shown in the lower panel of Fig. 6(a). $C(z)$ varies between 10 and 100 mm^{-1} over the modified (laser-drilled) region where the fiber core is affected. The coupling coefficient reduces quickly away from the center of the hole and becomes zero over the region where the fiber is undisturbed. This is expected because mode coupling over the unperturbed section of the fiber is prohibited due to mode orthogonality. When an array of periodically distributed holes is drilled along the PCF with a separation of several hundred microns, they form a "source" that drives phase-matched light to resonantly couple into co-propagating cladding local-modes. Since $C(z)$ is a periodic function of z, it can

#119793 - $15.00 USD Received 10 Nov 2009; revised 25 Dec 2009; accepted 4 Jan 2010; published 3 Mar 2010
(C) 2010 OSA

be expanded into a Fourier series $C(z) = \sum_N f_N \exp(i\frac{2\pi N}{\Lambda} z)$. When the phase-matching condition $N\lambda_{res} = \int_{z_0}^{z_0+\Lambda} \left[n_{co}(z,\lambda_{res}) - n_{cl}(z,\lambda_{res})\right] \cdot \mathrm{d}z \approx (n_{co} - n_{cl})\Lambda$ is satisfied, where n_{co} and n_{cl} are respectively the effective indexes of the core and cladding modes for the unperturbed PCF, resonant couplings are induced at the resonant wavelength λ_{res}. N = 1, 2, … correspond to the first, second, and higher order gratings. The calculated relationship between LP_{01} - LP_{11} resonant wavelength λ_{res} and the grating period Λ for N = 1 is shown as the solid black curve in Fig. 5. The close match between the calculated and the measured results confirms that the coupling is between the LP_{01} core mode and the LP_{11} cladding mode and the LPG is a first-order grating. With initial condition b_{co} (0) = 1 and b_{cl} (0) = 0, and the calculated $C(z)$ as shown in Fig. 6(a), Eq. (1) was solved numerically and the LPG transmission spectrums for different number of drilled holes are plotted in Fig. 6(b). As expected the depth of resonant dip increases with the number of holes and reaches to ~14 dB with 15 holes. Although the calculated transmission spectrums agree with the measured ones (Fig. 3) in trend, there is significant difference in the depths of the transmission dips. The discrepancy may be partly attributed to the inaccurate estimation of the geometrical parameters used in our model, but we believe that it may be mainly due to the limitation of the coupled local-mode theory. Compared with the simplified coupled mode theory, the coupled local-mode theory may be used to study mode-coupling with stronger waveguide perturbations. However, it is still derived under the assumption that the variation is slow over a fiber length of the wavelength scale. Since the drilled-holes in the present work introduce abrupt changes of the fiber geometry over a micrometer length scale, the coupled local-mode theory may not be applied to quantitatively predict the behavior of such LPGs.

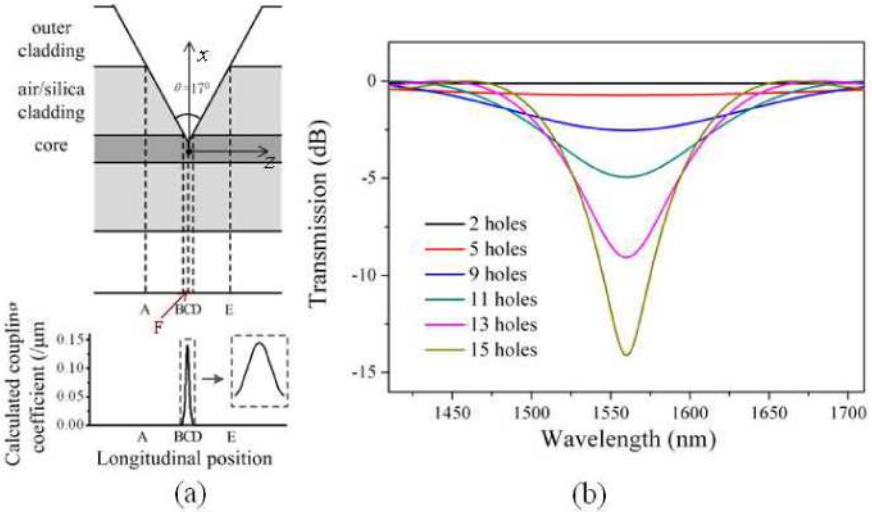

Fig. 6. (a) Side view of a single-hole model for the calculation of coupling coefficient and the calculated longitudinal variation of LP_{01}-LP_{11} coupling coefficient around the hole. (b) Calculated evolution of transmission spectrum with increasing number of drilled-holes. The parameters used in the calculation are: diameter of the air hole d = 3.38 μm, hole to hole spacing D = 7.31 μm, grating period Λ= 420 μm. Position F is located between B and C and is represented by z = –0.75 μm plane.

To fabricate good quality LPGs, several parameters need to be optimized. Firstly, to drill holes in the holey fiber cladding, the femtosecond laser intensity needs to be above certain threshold energy; however, if the laser intensity is too high, the enhanced micro-explosions cause roughness of the fiber surface and the diameter of the hole is enlarged. Secondly, the

#119793 - $15.00 USD Received 10 Nov 2009; revised 25 Dec 2009; accepted 4 Jan 2010; published 3 Mar 2010
(C) 2010 OSA

moving speed of the PCF in the x-direction determines the shape of holes and the machining efficiency. If the speed is high, the silica in the cladding is not removed completely. On the other hand, if the speed is too low, the excessive laser intensity will damage the peripheral silica of the holes, and the machining efficiency decreases [26]. In our experiment, the femtosecond pulse laser intensity and the moving speed of the translating stage used to drill the holes are 2.65×10^{15} W/cm^2 and 5 μm/s, respectively. These two parameters depend on each other and should be selected as a matched pair. This selection was achieved by a systematic experimental optimization guided by the cross-sectional image of the holes and the growth of the transmission dip of the fabricated LPGs. The air-columns in the PCF might cause scattering and redistribution of the femtosecond laser intensity; however, we found that they have no observable effect on the shape and the quality of the drilled holes for the selected drilling parameters.

For the LPG shown in Fig. 2, the drilled-holes is toward the center of the fiber, and only the even LP_{11} mode with their two lobes on the two sides of the $x = 0$ plane (as shown in Fig. 4(a)) are excited. For this LPG, although large PDL is measured, the splitting of the attenuation dips is not obvious (Fig. 3), indicating the polarization-related splitting of the resonant dip is not significant. If the drilled-hole deviates from $y = 0$ plane, splitting of the attenuation dip is observed, and the largest splitting can be as big as 30 nm. We believe that the large splitting is due to coupling to two LP_{11} modes (i.e., even and odd LP_{11}) with different intensity profiles. With a "tilted" hole that is not directed toward the center of the fiber, both even and odd LP_{11} modes will be excited. The odd LP_{11} mode has two lobes on the two sides of $y = 0$ plane and can have considerably different mode-index from the even LP_{11} mode, resulting in different resonant wavelengths. Therefore, it is important to make careful alignment in order to ensure a high quality LPG with a single attenuation dip. We also observed a difference of several nanometers between the resonant wavelengths among several LPGs fabricated under similar experimental conditions, probably due to the lack of repeatability of the positioning of the laser focus with respect to the optical fiber and slight differences in the periodicity of the grating that results. We found that, with our current experimental setup, it is difficult to ensure a perfect consistency when aligning the direction of the fiber with the moving direction of the translation stages, which may be one of the reasons responsible for the observed non-repeatability. However, this is only a first demonstration of the LPGs made by drilling holes in PCFs with a focus femtosecond laser. There is room for future research and improvements.

4. Conclusion

In conclusion, we reported the first fabrication of femtosecond-laser-drilled structural LPGs in a large-mode-area PCF. A compact LPG less than 4 mm in length was fabricated by drilling 10 holes in the cladding of the PCF. It exhibited a strong transmission dip of over 20 dB. The mode coupling process was explained by using the coupled local-mode theory. The theoretical results agree qualitatively with the measured transmission spectrum and the near-field output intensity profile of the LPG at the resonant wavelength. However, there is considerable discrepancy between the measured and calculated depths of the transmission dips. Further work is needed to accurately model the mode-coupling process by using a strong perturbation theory, and to study the response of the LPG to temperature, strain, bend, and external refractive index, etc., for the purpose of developing novel photonic devices and sensors.

Acknowledgements

The work is supported by Hong Kong SAR government through a GRF grant PolyU5182/07E, the Hong Kong Polytechnic University through grant J-BB9K, and NSF of China through grant 60629401.

#119793 - $15.00 USD Received 10 Nov 2009; revised 25 Dec 2009; accepted 4 Jan 2010; published 3 Mar 2010
(C) 2010 OSA